HHS Public Access

Author manuscript

*Nat Nanotechnol*. Author manuscript; available in PMC 2011 June 20.

Published in final edited form as:

*Nat Nanotechnol*. 2010 July ; 5(7): 545–551. doi:10.1038/nnano.2010.104.

# Sub-Cellular Resolution Delivery of a Cytokine via Precisely Manipulated Nanowires

**Donglei Fan**[1,2,4,*], **Zhizhong Yin**[3,5,*], **Raymond Cheong**[3], **Frank Q. Zhu**[2,6], **Robert C. Cammarata**[1], **C.L. Chien**[1,2,#], and **Andre Levchenko**[3,#]

[1] Department of Materials Science and Engineering, Johns Hopkins University, 3400 N. Charles St., Baltimore, MD 21218, USA

[2] Department of Physics and Astronomy, Johns Hopkins University, 3400 N. Charles St., Baltimore, MD 21218, USA

[3] Department of Biomedical Engineering, Johns Hopkins University, 3400 N. Charles St., Baltimore, MD 21218, USA

## Abstract

Precise delivery of molecular doses of biologically active chemicals to a pre-specified single cell among many, or a specific sub-cellular location, is still a largely unmet challenge hampering our understanding of cell biology. Overcoming this could allow unprecedented levels of cell manipulation and targeted intervention. Here, we show that gold nanowires conjugated with cytokine, such as tumour necrosis factor-alpha (TNFα), can be transported along any prescribed trajectory or orientation using electrophoretic and dielectrophoretic forces to a specific location with subcellular resolution. The nanowire, 6 μm long and 300 nm in diameter, delivered the cytokine and activated canonical nuclear factor-kappaB signaling in a single cell. Combined computational modeling and experimentation indicated that cell stimulation was highly localized to the nanowire vicinity. This targeted delivery method has profound implications for controlling signaling events on the single cell level.

---

Cells communicate via highly localized signals that are secreted by neighboring cells or transmitted via direct cell-cell contact [1–3]. Understanding these processes in natural and model experimental systems demands highly precise signal delivery with sub-cellular

---



[#]To whom correspondence should be sent: alev@jhu.edu, clc@pha.jhu.edu.
[*]These authors contributed equally to this work.
[4]Current address: Texas Materials Institute, Department of Mechanical Engineering, University of Texas at Austin, Austin, TX 78712 USA
[5]Current address: DNA Medicine Institute, 727 Massachusetts Ave, Cambridge, MA 02139, USA
[6]Current address: Hitachi Global Storage Technology, 3403 Yerba Buena Road, San Jose, CA 95135, USA

AUTHOR CONTRIBUTIONS

D.F., Z.Y., C.L.C, and A.L. conceived and designed the experiments and analysis. Z.Y., D.F., and F.Q.Z. performed the experiments and analyzed the data. R.C. performed the simulations. All authors discussed the results and co-wrote the paper.

ADDITIONAL INFORMATION

Supplementary information accompanies this paper at www.nature.com/naturenanotechnology. Reprints and permission information is available online at http://npg.nature.com/reprintsandpermissions/.

resolution. Recently, photoactivated release of caged molecules and photoactivation of biological molecules have helped to understand the local function of small signaling messengers (such as $Ca^{2+}$ and cyclic adenosine monophosphate) and larger signaling proteins [4–6]. However, photoactivatable substrates rely on chemistry that is highly specific to the molecule of interest, and require considerable optimization efforts. Microfluidic systems also affords precise delivery by allowing a sharp gradient of stimulant molecules to flow over target cells, but suffer from the adverse effects of flow-induced shear stress [7–9]. Moreover, the sharp gradient selectively stimulates only a small fraction of cells, leaving the majority of cells either fully stimulated or completely unstimulated.

Here we show that nanowires functionalized with molecular signals can deliver the payload to a pre-specified cell with subcellular resolution, without the use of specialized chemistry or continuous fluid flow. Because of their pronounced aspect ratio, nanowires have sizable and predictable dipole moments that can be manipulated by electric fields. Recently, we showed that by applying a combination of alternating and constant electric fields applied via lithographically patterned electrodes, nanowires can be moved along any arbitrary trajectory with speeds up to 50 μm/sec and positioned at an arbitrary location with a precision better than 300nm [10–13]. The alternating fields controlled the nanowire orientation while the constant fields controlled the direction of translation. Using this method (called ‘electric tweezers’), we now show that nanowires functionalized with the TNFα cytokine can target and deliver the payload to single cells among many. This cytokine has a small spatial range of action *in vivo*, since avoiding broad systemic action is essential for the prevention of potentially lethal complications, such as septic shock [14]. Thus, it is of considerable biological and clinical significance to deliver TNF α in a localized manner and determine the ensuing signaling response.

## Nanowire fabrication and manipulation by electric fields

We fabricated gold nanowires by electrodeposition through nanoporous templates [15] yielding cylindrically shaped particles 300 nm in diameter and 6 μm long. We used nanowires of this size to facilitate the observation of their motion by optical microscopy, even though we have successfully manipulated nanowires of far smaller sizes [11]. Nonetheless, the nanowires are far smaller than most eukaryotic cells (cf. 10 μm characteristic diameter for mammalian cells) enabling sub-cellular delivery resolution and facilitating transport through aqueous solutions (cf. equivalent Stokes diameter of 1.25 μm, see Methods). Their large 1:20 aspect ratio also allows precise manipulation using electrical fields [10–13]. In this study, we increased the hydrophobicity of the nanowire [16] by coating it with 1-dodecanethiol, thereby enabling hydrophobic surface mediated adsorption of TNFα from a concentrated solution (Fig. 1a). The adsorption of TNFα was confirmed by using rhodamine-conjugated TNFα (Fig. 1b). We note that the gold composition of the nanowires also allows surface functionalization using alternative techniques, enabling delivery of a wide variety of substances other than TNF α, as needed.

The isoelectric point of TNF α is 5.3, making it weakly negatively charged at neutral pH [17]. Thus, TNF α coating of the neutrally charged Au nanowires confers a negative charge in most cell growth media and isotonic buffers, enabling manipulation by electric fields. In a

constant electric field $\boldsymbol{E_{DC}}$, a nanowire with charge $q$ experiences an electrophoretic force of $q\boldsymbol{E_{DC}}$. Thus, the motion of a nanowire can be dictated by two sets of parallel electrodes (Fig. 1d) that provide uniform electric fields in the X and the Y directions. By controlling the magnitude and duration of the two electric field components, a nanowire can be compelled to move along any prescribed trajectory within the region bounded by the electrodes. Under an alternating non-uniform electric field $\boldsymbol{E_{AC}}$ a nanowire can be subjected to a dielectrophoretic (DEP) force, although if the applied $\boldsymbol{E_{AC}}$ is uniform, as is the case between parallel electrodes, no DEP force is generated. However, the nanowire can still be subjected to a torque $\boldsymbol{p} \times \boldsymbol{E_{AC}}$, exerted on the induced electric dipole $\boldsymbol{p}$, aligning the nanowires in the direction of $\boldsymbol{E_{AC}}$. Thus, simultaneously applying a uniform $\boldsymbol{E_{AC}}$ and a uniform $\boldsymbol{E_{DC}}$ enables transport of a nanowire in a prescribed direction or along a complex trajectory with a specific orientation (Fig. 1e and Supplementary Movie 1). The speed of nanowire movement is proportional to $|\boldsymbol{E_{DC}}|$, which for fixed electrodes was proportional to the applied voltage (Fig. 1f), in agreement with our previous work [10]. This enabled user-controlled velocities as high as 22 μm/sec at the voltage of about 3 V, from which we estimated by the Smoluchowski equation that the zeta potential of the nanowires is 69 mV [18]. We note that since, at low Reynolds numbers, both the zeta potential and opposing viscous forces primarily scale with the nanowire length but not diameter, we expect that nanowires with smaller diameters or lengths can be manipulated with electric fields of similar strength. These results indicated that functionalized nanowires could indeed be transported to a specific location with a high degree of precision.

To test whether the controlled transport of functionalized nanowires could enable delivery of immobilized TNFα to pre-specified cells or subcellular locations, we created wells for cell culture by placing a piece of polydimethylsiloxane (PDMS) with open chambers over the operating areas and surrounding electrodes (Fig. 1d). Following overnight culturing of HeLa cells in the chambers, the culture medium was temporarily replaced by a DEP medium [19] to allow electric control of nanowire movement. DEP medium is a non-ionic isoosmotic solution with small dielectric screening effect, so that the nanowires can be effectively manipulated onto specific live cells by electric fields [19]. The electric field conditions used to manipulate the nanowires (maximum field of 24V/mm for 2 min.) did not damage the cultured cells. Live/dead cell staining (Fig. 2a) showed that six hours after applying the electric field most cells in the culture area were viable (green) while dead cells (red) were confined to the area immediately adjacent to the electrodes, suggesting that the chosen conditions for nanowire manipulation were compatible with live cell experimentation.

To demonstrate that a single functionalized nanowire could indeed be transported onto a target cell using the electric field control, we selected a nanowire of interest in suspension, then applied a combination of AC (10 MHz, 5V) and DC (2V) electric fields, applied sequentially in the X and Y directions. Correspondingly, as it was gradually settling in the solution, the selected nanowire was aligned and transported in one direction, turned, and was transported in another direction before finally resting on the membrane of the cell (Fig. 2b, Supplementary Movie 2). The manipulation has submicron-level precision, so that a single nanowire could be maneuvered and reoriented over the cell surface in the span of a single cell, demonstrating the ability to target specific parts of the cell as desired (Fig. 2c,

Supplementary Movie 3). We found that the delivered nanowires adhered to the cell surface and did not move when electric fields were applied at the strength used to move the nanowires in solution. This property enabled us to sequentially transport one (Fig. 2d), two (Fig. 2e), and three (Fig. 2f) TNFα carrying nanowires onto the same pre-selected cell, by rapidly moving them from different locations in the nanowire suspension to the cell surface. Sequential transport of nanowires enables control over the amount of stimulant delivered to a cell, and more advantageously, enables the delivery of different stimuli at different times to the same cell or to neighboring cells.

## NF-κB signaling dynamics induced by TNF-conjugated nanowires

Canonically, TNFα exercises its cellular effects through NF-κB [20], a transcription factor normally kept in the cytosol through binding to inhibitory anchor proteins. NF-κB is released from the inhibitory proteins following TNFα receptor activation and translocates to the nucleus with complex kinetics [21]. Thus, visualizing the location of NF-κB can assist in the detection and analysis of TNFα signaling, such as cell signaling resulting from precise delivery of TNFα to cells via nanowires. We first visualized the translocation of NF-κB by immunocytochemical staining of p65, a subunit of NF-κB, following stimulation with 10ng/mL TNFα dissolved in the cell medium (an example of nuclear translocation visualized in this way is shown in Fig. 5b—compare the leftmost and rightmost panels). We observed NF-κB pathway activation kinetics commonly found in other cells types at this cytokine dose [21]: a rise to a peak at approximately 30 min. post-exposure, a drop to a trough at approximately 60 min. and then recovery to an intermediate level of a more persistent plateau (Fig. 3a, red squares).

We next examined NF-κB activation kinetics in cells stimulated with nanowires functionalized with TNFα. We incubated the cells with a 2–3mm thick solution of the nanowires, adjusting the concentration so that each cell was exposed to approximately 1–2 nanowires (Fig. 3b). For this cell medium height, direct microscopic observation indicated that nanowire sedimentation onto the cells was complete within 2 min., ensuring that cells were essentially simultaneously exposed to the nanowires as compared to the characteristic time of the NF-κB activation response determined above. When on the surface of the cells, the nanowires were not internalized and remained on the surface for at least 3 hrs, as determined by scanning electron microscopy and focused ion beam cross-sectioning (Supplementary Fig. 1). Immunocytochemical analysis of the response to TNFα delivered by nanowires showed that, in contrast to stimulation by TNFα dissolved in the medium, the NF-κB response was monophasic consisting of a single response peak with residual low level stimulation at 3 hrs. post-stimulus (Fig. 3a, blue circles). We confirmed the monophasic kinetics by examining NF-κB translocation in live HeLa cells expressing p65-GFP (Fig. 3a magenta circles, Fig. 3c-h, Supplementary Movie 4). On the other hand, stimulation with bare nanowires not carrying the adsorbed TNFα yielded no detectable response (Fig. 3a, black circles), demonstrating the specific role of the adsorbed TNFα.

The differences in the NF-κB dynamics in response to TNFα adsorbed on the nanowires versus TNFα dissolved in the medium indicated altered kinetics of TNFα availability in the cell microenvironment. Indeed, if the primary cell surface receptors that are stimulated are

those in contact with the nanowire, desorption of TNFα from the nanowires is expected to cause the amount of TNFα on the nanowire, and thus local cell stimulation, to decline in time. However, it is also possible that TNFα might diffuse to the cells from multiple nanowires through first enriching the cell supernatant, in which case the available TNFα and cell stimulation would increase in time. To distinguish these possibilities, we employed our extensive and experimentally validated computational model of the TNFα-mediated NF-κB activation [21], [22] in order to predict the TNFα input into the NF-κB pathway during nanowire stimulation that would trigger the observed NF-κB activation profile.

First, we demonstrated that the model can recapitulate the biphasic response to TNFα dissolved in the cell medium (orange curve in Figs. 4a, 4b and Supplementary Fig. 2), confirming the model applicability. Then, we considered the case in which the available TNFα increases in time, i.e., non-local cell stimulation through the supernatant. In the case of simple first-order desorption kinetics, we expect that the concentration of TNFα in the bulk medium to exponentially saturate [23] according to the form $c(t) = c_{os}\,[1 - \exp(-t/t_{os})]$ ($t > 0$) where $c_{os}$ is the limiting concentration and $t_{os}$ determines the rate of increase. We found that varying either of these two parameters simultaneously altered all three output features (Supplementary Fig. 2). We were unable to obtain a satisfactory fit due to a tradeoff between fitting the timing of the response peak and fitting the amplitude of the residual activity, suggesting that the observed dynamics are inconsistent with time-increasing delivery of desorbed TNFα via the bulk medium. Next, we examined whether the observed NF-κB dynamics could be explained by effective TNFα concentrations that decrease in time, i.e. due to localized cell stimulation. For this case, we tested inputs of the form $c(t) = u(t)\,c_{os}\exp(-t/t_{os})$. The unit step function $u(t)$ represents a sudden rise to an effective initial concentration of $c_{os}$ due to direct nanowire contact, followed by an exponential drop due to TNFα desorption and loss to the bulk medium at a rate determined by the time constant $t_{os}$. This family of input profiles produced excellent fits to the observed dynamics, with $c_{os}$ dictating the timing, and to a lesser degree, the amplitude of the NF-κB activation peak (Fig. 4a), and $t_{os}$ determining the residual activation levels (Fig. 4b). We found that the profile with $t_{os}$ = 2.00 hrs and and $c_{os}$ = 250 pg/mL (green curve in Fig. 4a and 4b) provided the optimal least squares fit to the experimental data (magenta circles in Fig. 4a and 4b). These results thus strongly suggested cell activation via local TNFα release from nanowires.

To test the predictions of the computational analysis, we measured TNFα desorption dynamics by performing an enzyme-linked immunosorbent assay (ELISA) to determine the concentration of TNFα released into the supernatant of a solution of nanowires. We observed a gradually increasing concentration profile (Fig. 4c) resulting from a concentrated solution of nanowires (i.e., 5-fold more concentrated than that used in the live cell experiments). The profile fit well to exponential release of TNFα from the nanowires of the form $c = c_o\,[1 - \exp(-t/t_o)]$, where the terminal TNFα concentration of $c_o$ = 47.3 pg/ml and time constant of $t_o$ = 1.87 ± 0.31 hr gave the best fit. Moreover, the correspondence, within measurement error, of the measured $t_o$ = 1.87 hr and predicted $t_{os}$ = 2.00 hr reinforced the conclusion of the computational analysis. That is, cell stimulation is governed by the local TNFα concentration that gradually decreases due to desorption, rather than by an increasing TNFα concentration in the nanowire supernatant. This conclusion was further supported by

comparison of the maximum (steady state) TNFα concentration released from the nanowires into the solution of ~10 pg/ml (i.e., 1/5 of $c_o$) versus the estimated maximum concentration in the nanowire vicinity of $c_{os}$ = 250 pg/ml.

## Localized cell stimulation by TNF-conjugated nanowires

Given the highly local nature of nanowire-based stimulation, we tested whether cells could be stimulated in an addressable fashion. Using live HeLa cells transfected to express p65-GFP, we observed NF-κB translocation in cells in contact with nanowires but not in adjacent cells that were not in contact with nanowires (Fig. 5a, Supplementary Movies 5 and 6). We conclude that stimulation from TNFα coated nanowires is highly localized and that the presence or absence of nanowires can be used to selectively stimulate a single cell among many.

Finally, we measured the nanowire dose response by exposing wildtype cells to no nanowires, a dilute solution of nanowires (~200,000 nanowires/ml, corresponding to ~0.3 nanowires/cell), or a concentrated solution (~1,000,000 nanowires/ml, corresponding to ~1.5 nanowires/cell). Using immunocytochemistry to measure nuclear NF-κB translocation in a high throughput not achievable by live cell imaging, we found that following 45 min. nanowire stimulation (Fig. 5b) the average cell response correlated with the dose of nanowires (Fig. 5c), suggesting that the amplitude of NF-κB signaling in single cells may be controlled via the number of delivered nanowires.

## Conclusions

Living cells are exquisitely sensitive to changes in their immediate chemical and mechanical environment [24–26]. We showed that such sensitive responses can be elicited by cytokine-carrying nanowires, whose movement and orientation can be precisely controlled by electric fields. As few as a single TNF-conjugated nanowire was sufficient to stimulate NF-κB translocation in a single cell, in a manner consistent with modeling predictions for highly localized TNFα delivery. Given the unusual dynamics of the signaling events, it is of interest to contrast these results with *in vivo* cell stimulation by TNFα. *In vivo*, TNFα is released by TACE/ADAM17 or other proteolytic enzymes from the cell surface of macrophages responding to the presence of infectious agents [27]. The amount of TNFα released thus is likely a function of the cytokine available on the cell surface, generating kinetics of release that might be qualitatively similar to the kinetics of desorption from nanowires, since in both cases the amount released at a given time is determined by the rate of release and the amount still available on the cell or nanowire surface. Therefore, the nanowire-based delivery might approximate *in vivo* stimulation better than the usually used persistent cell stimulation. Interestingly, our results suggest that TNFα-based communication between macrophages and target cells could be extremely localized, involving close apposition of cells delivering and receiving the signal. Conversely, widespread TNFα signaling resulting from TNFα diffusion over multiple cell diameters may require a considerable number of macrophages, and may also be limited through other mechanisms [14]. Our results further suggest that the long-term cell response, which affects

expression of late response genes controlled by NF-κB [21], might be primarily a function of the rate of TNFα secretion rather than the number of signaling macrophages.

Finally, we note that adsorption, a simple method to immoblize proteins, confers an electric charge to nanowires and enables electric fields to move the nanowires at high speeds and deliver the biological signals to cells with high precision. Due to the considerable flexibility of Au surface chemistry, a multitude of other immobilization methods can be easily explored, including photoactivatable release of immobilized molecules from the nanowire, to vary the nature and timing of the substances delivered from a single nanowire or on a set of sequentially delivered nanowires. Combining these functionalities can permit both stimulation at the cell surface and intracellular stimulation via nanowire penetration into live cells [28], [29], in a single experiment. Such nanowire-delivered agents can facilitate sub-cellular level of control of cell function, including cell polarization and movement. Thus, we anticipate that this technique will find extensive use in the cell biology and bioengineering areas, and affect how biologically active compounds are delivered to cells and cell groups in various *in vitro* and *in vivo* settings.

## METHODS

### Nanowire preparation and functionalization

The Au nanowires were fabricated by electrodeposition into nanoporous alumina templates in a three-electrode set up [30]. A thick Cu layer (~ 2 μm) sputtered at the back of the template served as the working electrode, Ag/AgCl served as a reference electrode, and a Pt mesh served as counter electrode. A DC voltage of −1V with reference to the Ag/AgCl was applied on the working electrode to reduce Au ions in the solution into Au metal inside the nanopores of the template. The size of the nanopores defined the diameter of the nanowires, whereas the length of the nanowires was controlled by the amount of total electrical charge passing through the circuit. After the electrodeposition, the nanowires were released in a 2M NaOH solution followed by two cycles of sonication and centrifugation in ethanol and deionized (DI) water. The nanowires were then dispersed and re-suspended in solutions such as DI water.

The suspended Au nanowires were conjugated with TNFα protein (Invitrogen) by hydrophobic interaction. First, the Au nanowire surface was functionalized and made hydrophobic by incubation in 5 mM 1-dodecanethiol (98%, Alfa Aesar Inc.) ethanol solution overnight. After centrifugation and resuspension twice in ethanol, once in DI water, and once in phosphate buffered saline (PBS), the nanowires were incubated in 10ng/ml TNFα in PBS solution for 3–4 hours at 4°C. The excess TNFα on the nanowires and in solution was washed away by the PBS solution. Protein adsorption was measured using nanowires prepared in a similar fashion, but incubated in a solution of TNFα labeled with rhodamine (labeling kit from Thermo Fisher Scientific).

### Device fabrication and operation for nanowire manipulation

Detailed procedures for device fabrication and operation for manipulating nanowires can be found in our previous work [10]. In brief, the microelectrodes used to manipulate nanowires

were fabricated by standard photolithography. A thin chromium (Cr) layer (typically 20 nanometers thick) was first deposited on a glass substrate as the adhesion layer, followed by the deposition of a gold (Au) layer of 120 nanometers. S1813 photoresist was used to transfer the electrode patterns onto a transparent mask (CAD/Art Services, Inc.) then to the metal layer. After the development of the photoresist, the Cr/Au layers were etched by their respective chemical etchants. Electric voltages were applied to these microelectrodes through custom designed circuits, which controlled the duration and sequence of the applied electric fields. A slab of polydimethylsiloxane (Sylgard 184, Corning) with ~5mm holes was placed over the glass to form a well to enable cell culture in the nanowire manipulating area. Finally, the area was coated with 10μg/ml of fibronectin (Sigma) for cell adhesion.

### Computational modeling of TNF-induced NF-κB dynamics

We simulated NF-κB activation dynamics using the 'consensus' version of our computational model of the TNF-NF-κB signaling pathway [22]. The backbone of this version is our original model of the pathway [21] augmented with IκBβ- and IκBε-mediated negative feedback [31] and a coarse-grained description of TNF-induced IKK activation [14]. The 'consensus' model is capable of recapitulating a wide variety of NF-κB dynamics in wildtype cells and cells deficient in one or more IκB isoforms in response to various durations of TNFα stimulation [14, 21, 31, 32]. As a control, we simulated NF-κB dynamics in response to a step input of 10ng/mL TNF. To simulate stimulation by TNF-coated nanowires, we considered TNFα inputs of the form $c(t) = u(t)\, c_{os}\, [1 - \exp(-t/t_{os})]$ (Supplementary Fig. 2) or $c(t) = u(t)\, c_{os} \exp(-t/t_{os})$ (Fig. 4a, 4b), where $u(t)$ is the unit step function, the variable $c_{os}$ respectively reflects the limiting or initial concentration, and $t_{os}$ reflects the rate of desorption [14]. Matlab R2006a (MathWorks) code is available upon request.

To quantitatively compare simulations and experiment, as shown in Fig. 4a and 4b, we determined the scaling factor to convert the experimental unit for NF-κB activity (normalized intensity, Fig. 3a) to the simulation unit for NF-κB activity (μM). The scaling factor value of 0.73μM gave the best least squares fit between the simulated and experimentally measured NF-κB response to a step input of 10ng/mL TNFα (orange curve and red squares, respectively, in Fig. 4a and 4b). Next, we scaled the NF-κB response to TNF-coated nanowire as measured in a transfected HeLa cell into the simulated units (magenta circles in Fig. 4a, 4b). Finally, by varying the values of $c_{os}$ and $t_{os}$ in a grid-like fashion, we determined that the values of $c_{os}$ = 0.25 ng/mL and $t_{os}$ = 2.00 hrs gave the global best fit in the least squares sense to the experimental time-course.

Additional methods (calculation of Stokes diameter, TNFα desportion kinetics, cell culture, immunocytochemistry, microscopy, and image analysis) can be found in the Supplementary Information.

## Supplementary Material

Refer to Web version on PubMed Central for supplementary material.

## Acknowledgments

The authors thank Dr. W. Greene of UCSF for providing the p65 plasmid, J. Wang for helping with cell transfection, X. Li for TNFα labeling, and Z. Wang for microplate scanning. D.F., F.Q.Z., C.L.C. acknowledge support from the National Science Foundation (DMR 0403849). R.C.C. acknowledges support from the National Science Foundation (DMR 0706178). Z.Y., R.C., and A.L. acknowledge the support from the National Institutes of Health (GM072024, RR020839). D.F. acknowledges start up support from University of Texas at Austin. R.C. acknowledges support from the Medical Scientist Training Program at Johns Hopkins University.

## References

1. Bray SJ. Notch signalling: a simple pathway becomes complex. Nat Rev Mol Cell Biol. 2006; 7:678–89. [PubMed: 16921404]
2. Delves PJ, Roitt IM. The immune system. First of two parts. N Engl J Med. 2000; 343:37–49. [PubMed: 10882768]
3. Nagata S. Fas ligand-induced apoptosis. Annu Rev Genet. 1999; 33:29–55. [PubMed: 10690403]
4. Wu YI, Frey D, Lungu OI, Jaehrig A, Schlichting I, et al. A genetically encoded photoactivatable Rac controls the motility of living cells. Nature. 2009; 461:104–8. [PubMed: 19693014]
5. Lee HM, Larson DR, Lawrence DS. Illuminating the chemistry of life: design, synthesis, and applications of “caged” and related photoresponsive compounds. ACS Chem Biol. 2009; 4:409–27. [PubMed: 19298086]
6. Mayer G, Heckel A. Biologically active molecules with a “light switch”. Angew Chem Int Ed Engl. 2006; 45:4900–21. [PubMed: 16826610]
7. Takayama S, McDonald JC, Ostuni E, Liang MN, Kenis PJ, et al. Patterning cells and their environments using multiple laminar fluid flows in capillary networks. Proc Natl Acad Sci U S A. 1999; 96:5545–8. [PubMed: 10318920]
8. Takayama S, Ostuni E, LeDuc P, Naruse K, Ingber DE, et al. Selective chemical treatment of cellular microdomains using multiple laminar streams. Chem Biol. 2003; 10:123–30. [PubMed: 12618184]
9. Takayama S, Ostuni E, LeDuc P, Naruse K, Ingber DE, et al. Subcellular positioning of small molecules. Nature. 2001; 411:1016. [PubMed: 11429594]
10. Fan DL, Cammarata RC, Chien CL. Precision transport and assembling of nanowires in suspension by electric fields. Appl Phys Lett. 2008; 92:093115.
11. Fan DL, Zhu FQ, Cammarata RC, Chien CL. Controllable high-speed rotation of nanowires. Phys Rev Lett. 2005; 94:247208.
12. Fan DL, Zhu FQ, Cammarata RC, Chien CL. Efficiency of assembling of nanowires in suspension by ac electric fields. Appl Phys Lett. 2006; 89:223115.
13. Fan DL, Zhu FQ, Cammarata RC, Chien CL. Manipulation of nanowires in suspension by AC electric fields. Appl Phys Lett. 2004; 85:4175.
14. Cheong R, Bergmann A, Werner SL, Regal J, Hoffmann A, et al. Transient IkappaB kinase activity mediates temporal NF-kappaB dynamics in response to a wide range of tumor necrosis factor-alpha doses. J Biol Chem. 2006; 281:2945–50. [PubMed: 16321974]
15. Whitney TM, Searson PC, Jiang JS, Chien CL. Fabrication and Magnetic Properties of Arrays of Metallic Nanowires. Science. 1993; 261:1316–1319. [PubMed: 17731862]
16. Huber DL, Manginell RP, Samara MA, Kim BI, Bunker BC. Programmed adsorption and release of proteins in a microfluidic device. Science. 2003; 301:352–4. [PubMed: 12869757]
17. Aggarwal BB, Kohr WJ, Hass PE, Moffat B, Spencer SA, et al. Human tumor necrosis factor. Production, purification, and characterization. J Biol Chem. 1985; 260:2345–54. [PubMed: 3871770]
18. White B, Banerjee S, O’Brien S, Turro NJ, Herman IP. Zeta-potential measurements of surfactant-wrapped individual single-walled carbon nanotubes. J Phys Chem C. 2007; 111:13684–13690.
19. Yin Z, Noren D, Wang CJ, Hang R, Levchenko A. Analysis of pairwise cell interactions using an integrated dielectrophoretic-microfluidic system. Mol Syst Biol. 2008; 4:232. [PubMed: 19096359]

20. Wajant H, Pfizenmaier K, Scheurich P. Tumor necrosis factor signaling. Cell Death Differ. 2003; 10:45–65. [PubMed: 12655295]
21. Hoffmann A, Levchenko A, Scott ML, Baltimore D. The IkappaB-NF-kappaB signaling module: temporal control and selective gene activation. Science. 2002; 298:1241–5. [PubMed: 12424381]
22. Cheong R, Hoffmann A, Levchenko A. Understanding NF-kappaB signaling via mathematical modeling. Mol Syst Biol. 2008; 4:192. [PubMed: 18463616]
23. Schwarz, JA.; Contescu, CI. Marcel Dekker. Vol. xvi. New York: 1999. p. 787
24. Mato JM, Losada A, Nanjundiah V, Konijn TM. Signal input for a chemotactic response in the cellular slime mold Dictyostelium discoideum. Proc Natl Acad Sci U S A. 1975; 72:4991–3. [PubMed: 174088]
25. Kim DH, Han K, Gupta K, Kwon KW, Suh KY, et al. Mechanosensitivity of fibroblast cell shape and movement to anisotropic substratum topography gradients. Biomaterials. 2009; 30:5433–44. [PubMed: 19595452]
26. Van Haastert PJ, Devreotes PN. Chemotaxis: signalling the way forward. Nat Rev Mol Cell Biol. 2004; 5:626–34. [PubMed: 15366706]
27. Black RA, Rauch CT, Kozlosky CJ, Peschon JJ, Slack JL, et al. A metalloproteinase disintegrin that releases tumour-necrosis factor-alpha from cells. Nature. 1997; 385:729–33. [PubMed: 9034190]
28. Cai D, Mataraza JM, Qin ZH, Huang Z, Huang J, et al. Highly efficient molecular delivery into mammalian cells using carbon nanotube spearing. Nat Methods. 2005; 2:449–54. [PubMed: 15908924]
29. Pearton SJ, Lele T, Tseng Y, Ren F. Penetrating living cells using semiconductor nanowires. Trends Biotechnol. 2007; 25:481–2. [PubMed: 17935806]
30. Zoski, CG. Handbook of electochemistry. Elsevier; UK: 2007.
31. Kearns JD, Basak S, Werner SL, Huang CS, Hoffmann A. IkappaBepsilon provides negative feedback to control NF-kappaB oscillations, signaling dynamics, and inflammatory gene expression. J Cell Biol. 2006; 173:659–64. [PubMed: 16735576]
32. Werner SL, Barken D, Hoffmann A. Stimulus specificity of gene expression programs determined by temporal control of IKK activity. Science. 2005; 309:1857–61. [PubMed: 16166517]

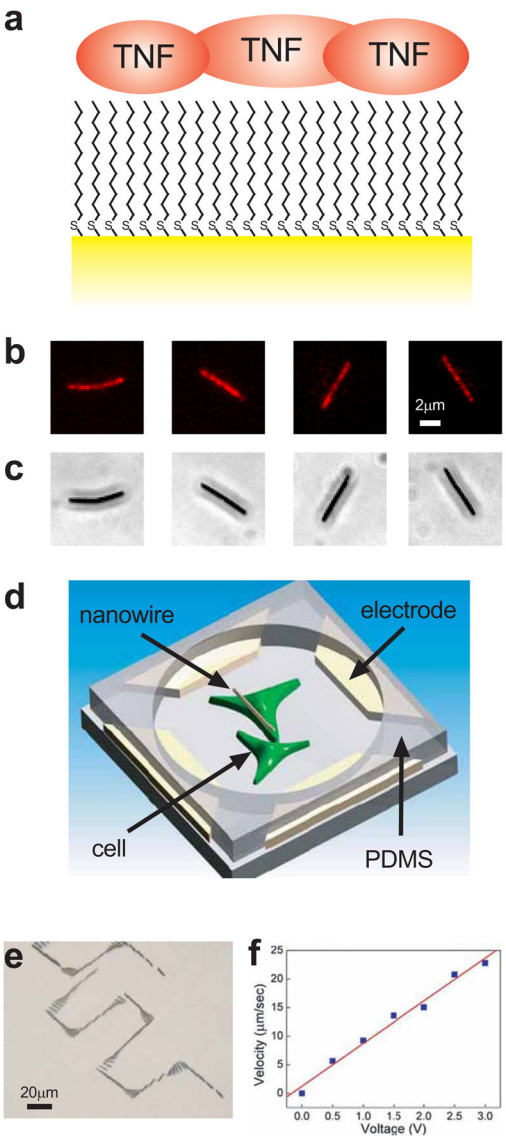


**Figure 1.**

Nanowire functionalization and movement. a, Schematic shows nanowire (yellow) surface modified with 1-dodecanethiol, rendering the surface hydrophobic and allowing the adsorption of TNF α (red). Fluorescent (b) and phase contrast (c) images of rhodamine-conjugated TNF α adsorbed on the surface of individual nanowires. d, Schematic shows two pairs of parallel electrodes that control nanowire orientation and movement by alternating and constant electric fields. PDMS placed over the electrodes forms a well in which cells are cultured. e, Overlay of a time series of phase contrast images showing the trajectory of the nanowires through precise rotations and translations (see also Supplementary Movie 1). f, Nanowire transport speed is proportional to the applied constant electric field, allowing precise control over nanowire velocity.

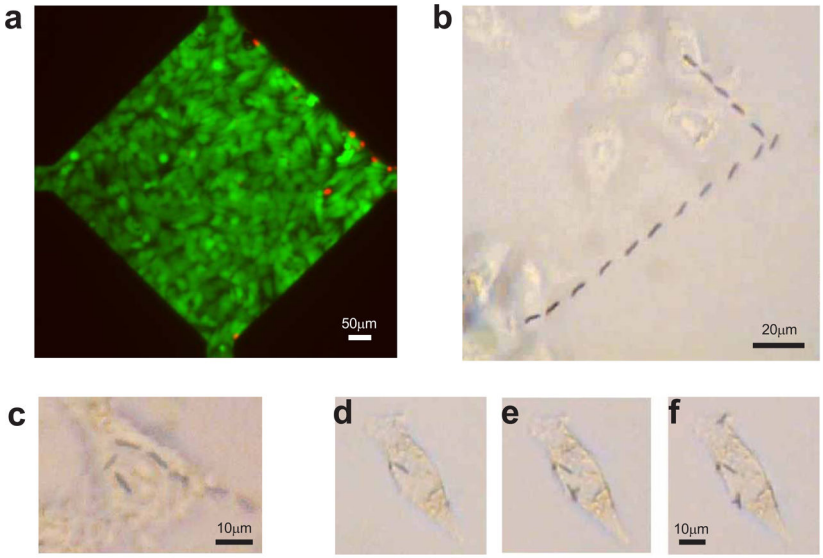


**Figure 2.**

Nanowire delivery to pre-selected cells. a, Live (green) and dead (red) cell staining showing that typical voltages used to manipulate nanowires does not affect the viability of most cells in the operating area. Dead cells were confined to the areas immediately adjacent to the electrodes. b, Overlay of a time series of phase contrast images showing delivery of a single nanowire to the cell at the top of the image. (See also Supplementary Movie 2.) c, Overlay of a time series of phase contrast images showing delivery of a single nanowire to sub-divisions of the same cell. (See also Supplementary Movie 3.) d–f, Phase contrast images showing sequential delivery of nanowires to a single cell.

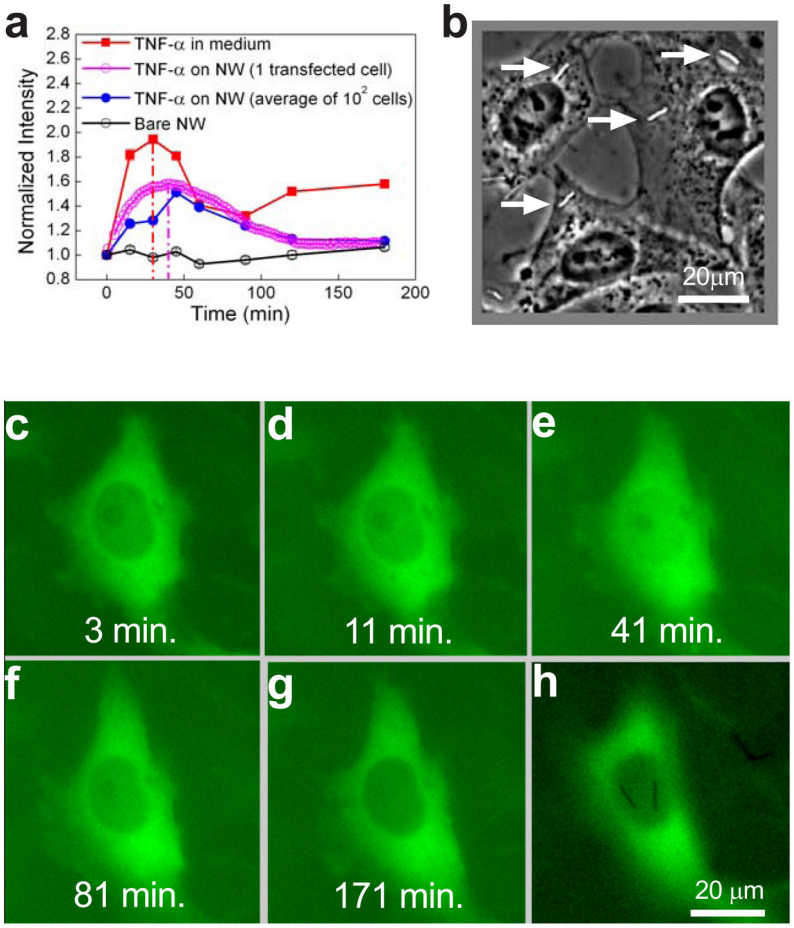


**Figure 3.**

Delivery of functional TNF α by nanowires. a, Average time-course of nuclear NF-κB concentration in wildtype HeLa cells exposed to 10ng/mL TNF α dissolved in the medium (red), TNF α-coated nanowires (blue), or bare nanowires (black) as measured by immunocytochemistry. Nuclear NF-κB measured in a HeLa cell expressing p65-GFP exposed to TNF α-coated nanowires is shown in magenta. b, Phase contrast image showing TNF α-coated nanowires (arrows) at a concentration that yielded ~1 nanowire per cell. c–h, Representative HeLa cell expressing p65-GFP stimulated with TNF α-coated nanowires for the indicated durations (panels c–g). Nuclear p65 levels peak around 40 min (see also Supplementary Movie 4). In panel h, the same cell is imaged at a different focal plane to show the two TNF α-coated nanowires that contact and stimulate the cell.

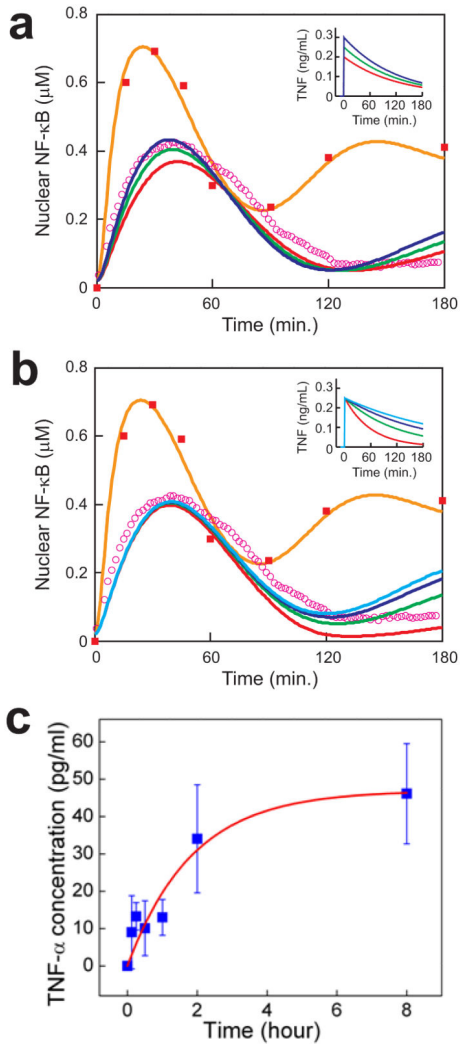


**Figure 4.**

Simulations predict localized TNF α delivery. a,b, The simulated response to 10ng/mL TNF α (orange) compares well with experiment (red squares, same as Fig. 3a). Simulated responses to TNF α inputs of the form $c(t) = c_{os} \exp(-t/t_{os})$ ($t > 0$) are shown. In panel a, $t_{os}$ = 120 min. and $c_{os}$ = 0.20 (red), 0.25 (green), 0.30 (blue) ng/mL. In panel b, $c_{os}$ = 0.25 ng/mL and $t_{os}$ = 60 (red), 120 (green), 180 (blue), 240 (light blue) min. The green curves give the best fit to experiment (magenta circles, same as Fig. 3a). See Methods for the model description. c, TNF α-desorption kinetics determined by ELISA measurements of TNF α concentration in the supernatant of a solution of $5\times10^6$ nanowires/mL. See text for description of the fitted exponential curve (red).

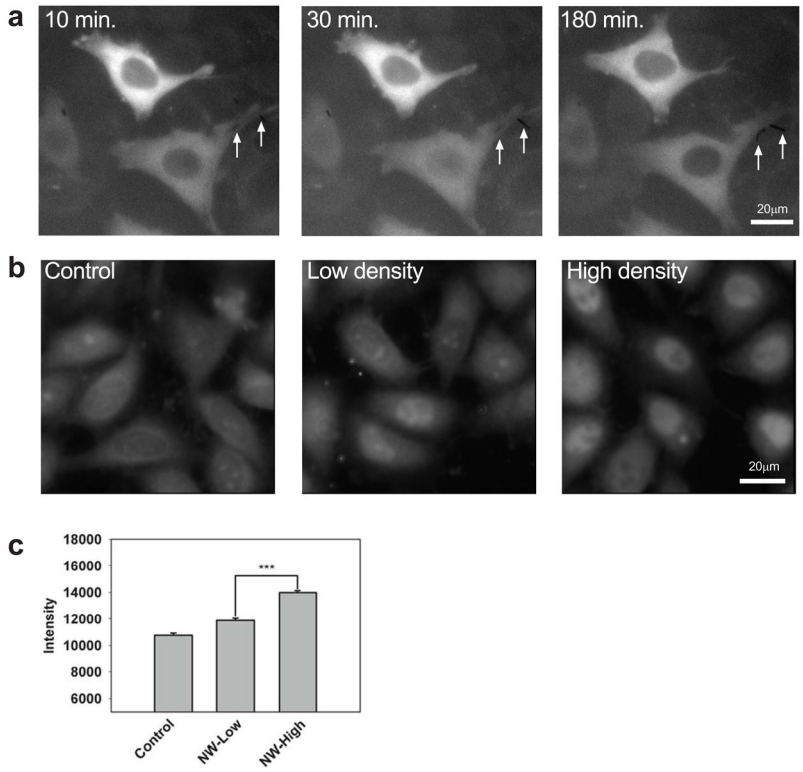


**Figure 5.**

Selective stimulation by TNF α-coated nanowires. a, HeLa cells expressing p65-GFP at the indicated times following stimulation with TNF α-coated nanowires. The lower cell contacts two nanowires (arrows) and exhibits p65 nuclear translocation whereas the upper cell contacts no nanowires and exhibits no translocation. (See also Supplementary Movie 5.) b,c, Wildtype HeLa cells stained for NF-κB following exposure to solutions of 0 (control), $0.2 \times 10^6$ (low density), or $1 \times 10^6$ (high density) TNF α-coated nanowires/mL, corresponding to 0, ~0.3, ~1.5 nanowires/cell on average, respectively. In (b), representative images are shown. In (c), the average NF-κB level is plotted (more than 150 cells measured for each condition). NF-κB levels were significantly different ($p < .001$) between the high and low stimulation cases.